



University of Bahrain  
**Journal of the Association of Arab Universities for  
 Basic and Applied Sciences**

[www.elsevier.com/locate/jaaubas](http://www.elsevier.com/locate/jaaubas)  
[www.sciencedirect.com](http://www.sciencedirect.com)



# Hall and ion slip effects on mixed convection flow of nanofluid between two concentric cylinders

D. Srinivasacharya \*, Md. Shafeeurr Rahman

*Department of Mathematics, National Institute of Technology Warangal 506004, India*

Received 29 October 2016; revised 28 January 2017; accepted 4 March 2017

## KEYWORDS

Magnetohydrodynamics;  
 Nanofluid;  
 Mixed convection;  
 Concentric cylinders;  
 Hall and ion-slip effects;  
 Homotopy analysis method

**Abstract** This article analyzes the effects of Hall and ion-slip parameters on mixed convective electrically conducting nanofluid flow between two parallel concentric cylinders considering magnetic field. The governing equations are non dimensionalized. The resulting system of nonlinear ordinary differential equations is solved utilizing homotopy analysis method. The influence of the magnetic parameter, Hall, ion-slip, Brownian motion and thermophoresis parameters on non-dimensional velocity, temperature and nanoparticle volume fraction is analyzed and represented graphically. It is found that increasing Hall and ion-slip parameters decrease the temperature but increase the velocity and nanoparticle volume fraction and the opposite trend observed when magnetic parameter increased. It is observed that as Brownian motion and thermophoresis parameters increase, the velocity and temperature increase but the nanoparticle volume fraction decreases.

© 2017 University of Bahrain. Publishing services by Elsevier B.V. This is an open access article under the CC BY-NC-ND license (<http://creativecommons.org/licenses/by-nc-nd/4.0/>).

## 1. Introduction

The analysis of heat transfer and mixed convection flow in an annular region between two concentric cylinders has been concentrating on vast investigation for many years. This is because of its wide range of applications in the model of cooling devices for microelectronic and electronic equipment, solar energy collection, etc. A number of investigations have been reported on the convective heat transfer flows in the annulus region between two concentric cylinders (See Dawood et al. (2015) for review of such flows). Nanofluids are intermission of nanoparticles in a mixed conventional fluid Choi and Eastman (1995). Nanofluids, first pioneered by Choi and

Eastman (1995), consist of uniformly dispersed and suspended nanometer sized particles in a base fluid. It has been established experimentally that these fluids have a thermal conductivity more than the base fluids. Nanofluids have applications in microelectronics, micro fluidics, transportation, biomedical, X-rays, material processing and scientific measurement. Buongiorno proposed an analytical model for convective transport in nanofluids, which incorporate the effects of Brownian diffusion and thermophoresis. Brownian motion and thermophoresis of nanoparticles were considered as the most probable mechanisms. The arbitrary motion of nanoparticles within the base fluid is called Brownian motion and this results from continuous collisions between the nanoparticles and the molecules of the base fluid. Brownian motion of nanoparticles constitutes a key mechanism of the thermal conductivity enhancement with increasing temperature and decreasing nanoparticle size with no effect in heat transfer of nanofluids. The phenomenon in which the particles can diffuse under the

\* Corresponding author.

E-mail addresses: [dsc@nitw.ac.in](mailto:dsc@nitw.ac.in), [dsrinivasacharya@yahoo.com](mailto:dsrinivasacharya@yahoo.com) (D. Srinivasacharya).

Peer review under responsibility of University of Bahrain.

<http://dx.doi.org/10.1016/j.jaubas.2017.03.002>

1815-3852 © 2017 University of Bahrain. Publishing services by Elsevier B.V.

This is an open access article under the CC BY-NC-ND license (<http://creativecommons.org/licenses/by-nc-nd/4.0/>).

influence of a temperature gradient is called thermophoresis. The thermophoresis force tends to move the particles in the direction opposite to the temperature gradient, and in contrast, the Brownian motion force tends to move the particles from high concentration to low concentration areas of the fluid. Due to Brownian diffusion and thermophoresis the nanoparticles can move homogeneously with the fluid but they also possess a slip velocity relatively to the fluid. Several investigators analyzed the heat transfer and mixed convection flow of nanofluids in an annular region under various aspects. A numerical study of mixed convection of nanofluid in a concentric annulus with rotating inner cylinder is studied by Sheikhzadeh et al. (2013). Togun et al. (2014) presented a detailed review on convective heat transfer of fluid and nanofluid flow through various annular passage configurations with different boundary conditions for various fluids. Jamshad and Tauseefmohyuddin (2014), Tauseefmohyuddin et al. (2015), Tauseefmohyuddin and Irfanullahkhan (2016) and Zulfiqar et al. Zulfiqar and Tauseefmohyuddin (2016) analyzed heat and mass transfer analysis for the flow of a nanofluid between rotating parallel plates. Kandelousi and Ellahi (2015), Sheikholeslami and Ellahi (2015a,b), Sheikholeslami et al. (2016) studied the influence of induced magnetic field on free and mixed convective heat transfer of nanofluid. Naveed et al. (2016) numerically investigated the flow and heat transfer of nanofluid in an asymmetric channel with expanding and contracting walls suspended by carbon nanotubes. Aggregation effects on water base nanofluid over permeable wedge in mixed convection and the influence of induced magnetic field and heat flux with the suspension of carbon nanotubes for the peristaltic flow in a permeable channel studied by Akbar et al. (2015), Ellahi et al. (2015), Ellahi et al. (2016) Mojtab et al. (2016), Rahman et al. (2016) and Rashidi et al. (2015). Heat transfer effects on carbon nanotubes suspended nanofluid flow in a channel with non-parallel walls under the effect of velocity slip boundary condition is numerically studied by Irfanullahkhan et al. (2015), Umar et al. (2015, 2016).

Convection and heat transfer using nanofluids has acquired considerable attention in present days. It is due to their diverse application in scientific, engineering and industrialized applications such as cooling of nuclear reactor, power generating systems, automobile engines, welding equipment and heat exchanging in electronics devices. The convective heat transfer and fluid flow problems with the interaction of magnetic field have attracted much attention due to several astrophysics and industrial applications. Chamkha et al. (2015) presented a review on various research work done on the MHD convection of nanofluids in various geometries and applications. Mozayyeni and Rahimi (2012) studied the effect of the magnetic field applied in the radial direction on the mixed convective flow in a cylindrical annulus with rotating outer cylinder. Ashorynejad et al. (2013) studied numerically the mixed convective heat transfer in an annuli of horizontal cylinder filled with nanofluid considering constant radial magnetic field on the fluid. Omid et al. (2013) obtained an analytical solution to the influence magnetite field on mixed convective in an annuli. Sheikholeslami and Abelman (2015) studied the heat and mass transfer of nanofluid flow between two coaxial cylinders considering magnetic field. Das et al. (2015) analyzed the mixed convective nanofluids flow in a concentric cylindrical pipes considering a uniform magnetic field.

In the investigations concerned with the MHD convective flows, the Hall current and ion slip terms in Ohm's law were neglected in order to simplify the mathematical analysis of the problem. However, the significance of Hall current and ion slip are essential in the existence of strong magnetic field. Therefore, in several physical situations it is required to include the influence of Hall current and ion slip terms in the MHD equations. The effects of the Hall current on electrically conducting steady viscous fluid in channels was studied by Tani (1962). Srinivasacharya and Kaladhar (2012, 2013) studied the effects of Hall current, the ion slip effect on mixed convective couple stress fluid flow between two circular cylinders. Garget et al. Garg et al. (2014) investigated the impact of Hall parameter on oscillatory convective viscoelastic magnetohydrodynamic flow in a vertical channel. Hayat et al. (2016) addressed the effects of Hall and ion slip, radiation and viscous dissipation on the mixed convective flow of nanofluid in a channel.

The literature survey reveals that the problem on mixed convective heat transfer flow of nanofluid in a concentric cylinders considering the impact of Hall current, ion slip parameter has not been considered. Also, the interaction of Hall current, ion slip influence with magnetite nanoparticles in a mixed convective flow, presents an interesting fluid dynamics problem. Hence, the aim of this paper is finding the impact of the Hall and ion slip parameter on the heat transfer flow of steady mixed convection nanofluid in a concentric cylinders. The homotopy analysis procedure is used to find the solution of ordinary differential equations. The HAM method, developed by Liao (2003), is a powerful technique to solve the various types of strongly non-linear equations. The effect of flow parameters on the velocity, temperature, nanoparticle volume fraction are examined.

## 2. Formation of the problem

Let the steady, laminar and incompressible nanofluid flow in the annular space between two infinitely long concentric cylinders of radius  $a$  and  $b$  ( $a < b$ ) and kept at temperatures  $T_a$  and  $T_b$  respectively. Choose a cylindrical polar coordinate system  $(r, \phi, z)$  with  $z$ -axis along the common axis of the cylinders (as shown in Fig. 1) and  $r$  normal to the  $z$ -axis. Assume that the outer cylinder is rotating with a constant angular velocity  $\Omega$  whereas the inner cylinder is at rest. The flow is generated because of the rotation of the exterior cylinder. Since the flow is fully developed and the cylinders are of infinite length, the flow depends only on  $r$  and a strong magnetite field  $B_0$  is imposed in an axial direction. The induced magnetic field is ignored with the presumption of the magnetic Reynolds number is very low. Assume relatively high electron-atom collision frequency so that the impact of Hall, ion slip cannot be omitted. Thermophysical characteristics of the nanofluid are taken as constant except density in the buoyancy term of the momentum equation. The flow is a mixed convection flow taking place under thermal buoyancy and uniform pressure gradient in azimuthal direction. The velocity component along  $\phi$  direction, temperature and nanoparticle volume fraction are denoted by  $u$ ,  $T$  and  $\phi$ , respectively. With the above assumptions and Boussinesq approximations with energy, the equations governing the steady flow of an incompressible nanofluid Buongiorno (2006) are

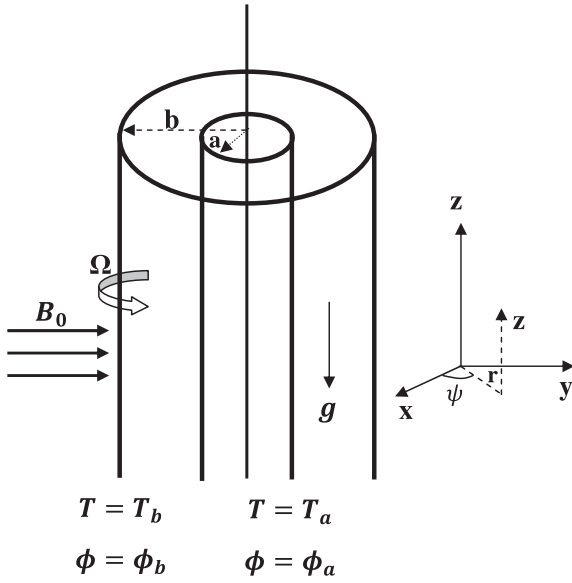


Figure 1 Geometry of the problem.

$$\frac{\partial u}{\partial \varphi} = 0, \quad (1)$$

$$\frac{\partial p}{\partial r} = \frac{u}{r^2} - \frac{\sigma B_0^2 \beta_h u}{(\alpha_e^2 + \beta_h^2)}, \quad (2)$$

$$\mu \nabla_1^2 u + (1 - \phi) \rho_f g \beta_T (T - T_a) - (\rho_p - \rho_f) g (\phi - \phi_a) - \frac{\sigma B_0^2 \alpha_e u}{(\alpha_e^2 + \beta_h^2)} - \frac{1}{r} \frac{\partial p}{\partial \varphi} = 0, \quad (3)$$

$$\alpha \left[ \frac{\partial^2 T}{\partial r^2} + \frac{1}{r} \frac{\partial T}{\partial r} \right] + \frac{\mu}{(\rho c)_p} \left[ \left( \frac{\partial u}{\partial r} \right)^2 - 2 \frac{u}{r} \frac{\partial u}{\partial r} + \left( \frac{u}{r} \right)^2 \right] + \tau \left[ D_B \frac{\partial T}{\partial r} \frac{\partial \phi}{\partial r} + \frac{D_T}{T_0} \left( \frac{\partial T}{\partial r} \right)^2 \right] = 0, \quad (4)$$

$$D_B \left[ \frac{\partial^2 \phi}{\partial r^2} + \frac{1}{r} \frac{\partial \phi}{\partial r} \right] + \frac{D_T}{T_0} \left[ \frac{\partial^2 T}{\partial r^2} + \frac{1}{r} \frac{\partial T}{\partial r} \right] = 0. \quad (5)$$

where the density is  $\rho$ , the pressure is  $p$ , the specific heat capacity is  $C_p$ , the viscosity coefficient is  $\mu$ , the acceleration due to gravity is  $g$ , the electrical conductivity is  $\sigma$ , ion slip parameter is  $\beta_i$ , Brownian diffusion coefficient is  $D_B$ ,  $\alpha_e = 1 + \beta_h \beta_i$  is a constant, the coefficients of thermal expansion is  $\beta_T$ , Hall parameter is  $\beta_h$ , the effective thermal diffusivity is  $\alpha$ , the thermophoretic diffusion coefficient is  $D_B$ , the coefficient of thermal conductivity is  $K_f = \alpha(\rho C_p)$ , the mass diffusivity is  $D$  and the mean fluid temperature is  $T$  and  $\nabla_1^2 u = \frac{\partial}{\partial r} \left[ \frac{1}{r} \frac{\partial}{\partial r} (ru) \right]$ .

The boundary conditions are:

$$u = 0, T = T_a, \phi = \phi_a \text{ at } r = a, \quad (6a)$$

$$u = b\Omega, T = T_b, \phi = \phi_b \text{ at } r = b. \quad (6b)$$

Introducing the following non-dimensional variables

$$\lambda = \frac{r^2}{b^2}, f(\lambda) = \frac{u\sqrt{\lambda}}{\Omega}, \theta = \frac{T - T_a}{T_b - T_a}, S = \frac{\phi - \phi_a}{\phi_b - \phi_a}, P = \frac{bp}{\mu\Omega}. \quad (7)$$

in Eqs. (1)–(5), we get the nonlinear differential equations as

$$4f''\lambda + \sqrt{\lambda} \frac{Gr}{Re} (\theta - NrS) - \frac{Ha^2 \alpha_e f}{\alpha_e^2 + \beta_h^2} - A = 0, \quad (8)$$

$$\lambda^3 \theta'' + \lambda^2 \theta' + Br \left[ \lambda^2 (f')^2 - 2\lambda f f' + (f)^2 \right] + Pr Nb \lambda^3 \theta' S' + Pr Nt \lambda^3 (\theta')^2 = 0, \quad (9)$$

$$\lambda S'' + S' + \frac{Nt}{Nb} (\lambda \theta'' + \theta') = 0. \quad (10)$$

where the prime indicate derivative corresponding to  $\lambda$ , the Prandtl number is  $Pr = \frac{\mu C_p}{k_f}$ , Grashof number is  $Gr = \frac{(1-\phi) g \beta_T (T_b - T_a) b^3}{\nu^2}$ , Reynold's number is  $Re = \frac{\rho \Omega b}{\mu}$ , constant pressure gradient is  $A = \frac{\partial P}{\partial \varphi}$ , Hartman number is  $Ha^2 = \frac{\sigma B_0^2 b^2}{\mu}$ , Brinkman number is  $Br = \frac{\mu \Omega^2}{k_f (T_b - T_a)}$ , Brownian motion parameter is  $Nb = \frac{\tau D_B (\phi_b - \phi_a)}{\nu}$ , thermophoresis parameter is  $Nt = \frac{\tau D_T (T_b - T_a)}{T_a \nu}$  and buoyancy ratio is  $Nr = \frac{(\rho_p - \rho_f)(\phi_b - \phi_a)}{\rho_f \beta_T (T_b - T_a)(1-\phi)}$ .

The corresponding boundary conditions (6) are

$$\begin{aligned} S = 0, \theta = 0, f = 0 \text{ at } \lambda = \lambda_0, \\ S = 1, \theta = 1, f = b \text{ at } \lambda = 1. \end{aligned} \quad (11)$$

### 3. Homotopy solution

The first step in HAM solution, is choosing the initial value of  $f(\lambda)$ ,  $\theta(\lambda)$  and  $S(\lambda)$  and auxiliary linear operators. (For more details on homotopy analysis method see the works of Liao (2003, 2004, 2010, 2013)). Therefore, we choose the initial approximations as

$$f_0(\lambda) = \frac{b(\lambda - \lambda_0)}{1 - \lambda_0}, \quad \theta_0(\lambda) = \frac{\lambda - \lambda_0}{1 - \lambda_0} \quad \text{and} \quad S_0(\lambda) = \frac{\lambda - \lambda_0}{1 - \lambda_0}. \quad (12)$$

and the auxiliary linear operators as

$$L_i = \frac{\partial^2}{\partial \lambda^2} \quad \text{for } i = 1, 2, 3. \quad (13)$$

such that

$$L_1(c_1 + c_2\lambda) = 0, \quad L_2(c_3 + c_4\lambda) = 0 \quad \text{and} \quad L_3(c_5 + c_6\lambda) = 0. \quad (14)$$

where  $c_j$ , ( $j = 1, 2, \dots, 6$ ), are constants. The second step in HAM is to defining the zeroth order deformation, which is given by

$$(1-p)L_1[f(\lambda; p) - f_0(\lambda)] = ph_1 N_1[f(\lambda; p)], \quad (15)$$

$$(1-p)L_2[\theta(\lambda; p) - \theta_0(\lambda)] = ph_2 N_2[\theta(\lambda; p)], \quad (16)$$

$$(1-p)L_3[S(\lambda; p) - S_0(\lambda)] = ph_3 N_3[S(\lambda; p)]. \quad (17)$$

where

$$N_1[f(\lambda, p), \theta(\lambda, p), S(\lambda, p)] = 4f''\lambda + \sqrt{\lambda} \frac{Gr}{Re} (\theta - NrS) - \frac{Ha^2 \alpha_e f}{\alpha_e^2 + \beta_h^2} - A, \quad (18)$$

$$N_2[f(\lambda, p), \theta(\lambda, p), S(\lambda, p)] = \lambda^3 \theta'' + \lambda^2 \theta' + Br \left[ \lambda^2 (f')^2 - 2 \lambda f f' + (f)^2 \right] + Pr Nb \lambda^3 \theta' S' + Pr Nt \lambda^3 (\theta')^2, \quad (19)$$

$$N_3[f(\lambda, p), \theta(\lambda, p), S(\lambda, p)] = S'' + S' + \frac{Nt}{Nb} (\lambda \theta'' + \theta'). \quad (20)$$

where  $p \in [0, 1]$  is the embedded parameter and  $h_j$ , ( $j = 1, 2, 3$ ) are auxiliary parameters which are not vanish.

The equivalent B.c's are

$$\begin{aligned} f(0; p) &= 0, & \theta(0; p) &= 0, & S(0; p) &= 0, \\ f(1; p) &= b, & \theta(1; p) &= 1, & S(1; p) &= 1. \end{aligned} \quad (21)$$

Next, the deformation equations of  $m^{th}$ -order are given by

$$L_1[f_m(\lambda) - \chi_m f_{m-1}(\lambda)] = h_1 R_m^f(\lambda), \quad (22)$$

$$L_2[\theta_m(\lambda) - \chi_m \theta_{m-1}(\lambda)] = h_2 R_m^\theta(\lambda), \quad (23)$$

$$L_3[S_m(\lambda) - \chi_m S_{m-1}(\lambda)] = h_3 R_m^S(\lambda). \quad (24)$$

where

$$\left. \begin{aligned} R_m^f(\lambda) &= 4f''\lambda + \sqrt{\lambda} \frac{Gr}{Re} (\theta - NrS) - \frac{Ha^2 \alpha_c f}{2\epsilon^2 + \beta_h^2} - A, \\ R_m^\theta(\lambda) &= \lambda^3 \theta'' + \lambda^2 \theta' + Br \left[ \lambda^2 (f')^2 - 2 \lambda f f' + (f)^2 \right] \\ &\quad + Pr Nb \lambda^3 \theta' S' + Pr Nt \lambda^3 (\theta')^2, \\ R_m^S(\lambda) &= S'' + S' + \frac{Nt}{Nb} (\lambda \theta'' + \theta'). \end{aligned} \right\} \quad (25)$$

for integer  $m$

$$\begin{aligned} \chi_m &= 0 & \text{for } m \leq 1, \\ &= 1 & \text{for } m > 1. \end{aligned}$$

From  $p = 0$  to  $p = 1$ , we can have

$$f(\lambda; 0) = f_0, \quad f(\lambda; 1) = f(\lambda), \quad (26)$$

$$\theta(\lambda; 0) = \theta_0, \quad \theta(\lambda; 1) = \theta(\lambda), \quad (27)$$

$$S(\lambda; 0) = S_0, \quad S(\lambda; 1) = S(\lambda). \quad (28)$$

Thus, as  $p$  varying from 0 to 1,  $f, \theta$  and  $S$  varies continuously from  $f_0, \theta_0$  and  $S_0$  to final value  $f(\lambda), \theta(\lambda)$  and  $S(\lambda)$  respectively. Using Taylor's series and Eq. (26),  $f, \theta$  and  $S$  can be written as

$$\begin{aligned} f(\lambda; p) &= f_0 + \sum_{m=1}^{\infty} f_m(\lambda) p^m, & f_m(\lambda) &= \frac{1}{m!} \frac{\partial^m f(\lambda; p)}{\partial p^m} \Big|_{p=0}, \\ \theta(\lambda; p) &= \theta_0 + \sum_{m=1}^{\infty} \theta_m(\lambda) p^m, & \theta_m(\lambda) &= \frac{1}{m!} \frac{\partial^m \theta(\lambda; p)}{\partial p^m} \Big|_{p=0}, \\ S(\lambda; p) &= S_0 + \sum_{m=1}^{\infty} S_m(\lambda) p^m, & S_m(\lambda) &= \frac{1}{m!} \frac{\partial^m S(\lambda; p)}{\partial p^m} \Big|_{p=0}. \end{aligned} \quad (29)$$

We have to choose the values of the auxiliary parameters for which the series (29) are converge at  $p = 1$  i.e.,

$$f(\lambda) = f_0 + \sum_{m=1}^{\infty} f_m(\lambda), \quad \theta(\lambda) = \theta_0 + \sum_{m=1}^{\infty} \theta_m(\lambda), \quad S(\lambda) = S_0 + \sum_{m=1}^{\infty} S_m(\lambda). \quad (30)$$

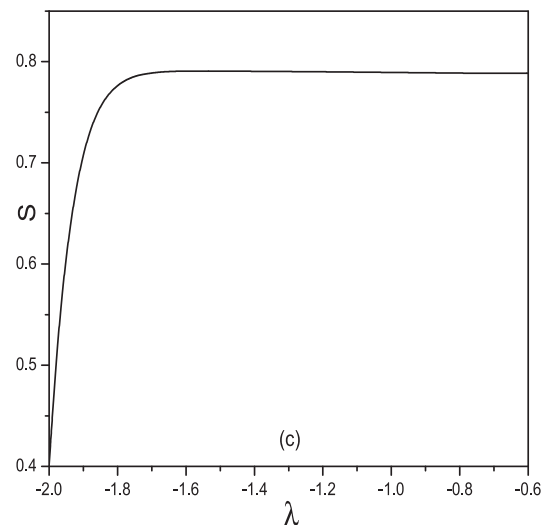
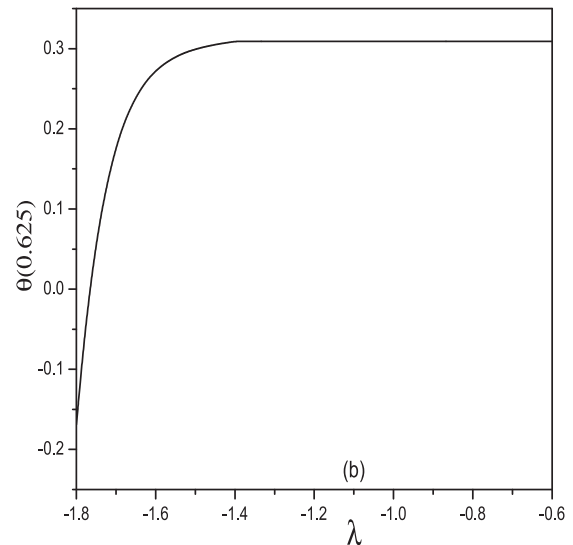
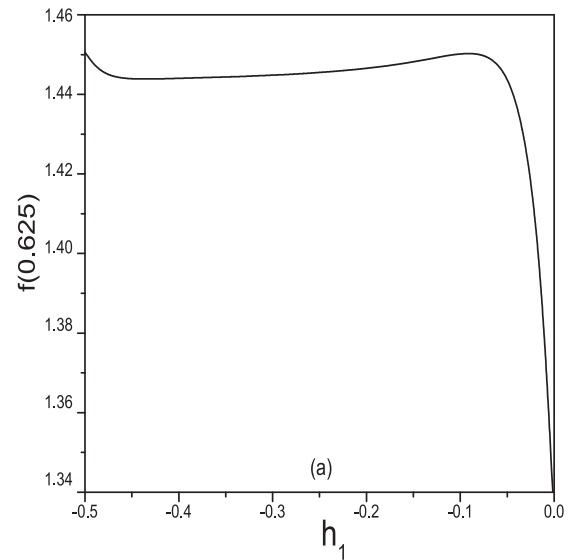


**Figure 2** The  $h$ -curves of  $f(\lambda), \theta(\lambda)$  and  $S(\lambda)$  when  $Nr = 1.0$ ,  $Nt = 0.5$ ,  $Nb = 0.5$ ,  $Gr = 10.0$ ,  $Ha = 5.0$ ,  $A = 1.0$ ,  $Re = 2.0$ ,  $Pr = 1.0$ ,  $\beta_i = 5.0$ ,  $\beta_h = 2.0$ ,  $Br = 0.5$ .

#### 4. Results and discussion

In HAM, it is essential to see that the series solution converges. Also, the rate of convergence of approximation for the HAM solution mainly calculate on the values of  $h$ . To find the admissible space of the auxiliary parameters,  $h$  curves are drawn for 16<sup>th</sup>-order of approximation and shown in Fig. 2. It is visible from these figures that the permissible interval for  $h_1, h_2$  and  $h_3$  is  $-0.5 < h_1 < -0.05, -1.0 < h_2 < -0.5$  and  $-1.8 < h_3 < -0.6$ , respectively.

In order to assess the accuracy of HAM method, we have compared our results with the analytical solution of Sinha and Chaudhary (1966), as well as the spectral quasilinearization method (SQLM) of Srinivasacharya and Himabindu (2016) in the absence of  $Gr, Ha, A, Pr, Nt$  and  $Nb$ . The comparison in the above case is found to be in good agreement, as shown in Table 1.

To obtain the optimal value of auxiliary parameters, the average residual errors (Ref. Liao (2010)) are computed and found that the average residual errors are least at  $h_1 = -0.43, h_2 = -0.67$  and  $h_3 = -1.60$ . Therefore, the optimality of convergence control parameters are appropriated as  $h_1 = -0.43, h_2 = -0.67$  and  $h_3 = -1.60$ . For different values of  $m$  the series solutions are calculated and represented in Table 2. It is noticed that the series (29) converges in the total area of  $\lambda$ .

The influence of magnetic parameter  $Ha$ , thermophoresis  $Nt$ , Brownian motion  $Nb$ , Hall-parameter  $\beta_h$ , ion slip  $\beta_i$  on the non-dimensional velocity  $f(\lambda)$ , temperature  $\theta(\lambda)$  and nanoparticle volume fraction  $S(\lambda)$  are shown graphically in Figs. 3–7 by taking the remaining parameters as  $Br = 0.5, Pr = 1.0, Gr = 10, A = 1, Re = 2, Nt = 0.5, Nb = 0.5$  and  $Nr = 1.0$ .

Fig. (3) represents the impact of the magnetite parameter  $Ha$  on dimensionless velocity in flow direction, temperature and nanoparticle volume fraction. Fig. (3a) reveals that the dimensionless velocity decays with a rise in  $Ha$ . The transverse magnetite field which is applied orthogonally to the direction of flow gives a resistive force known as Lorentz force. This Lorentz force resists the flow of nanofluid therefore the velocity decreases. Fig. (3b) illustrates the dimensionless temperature  $\theta(\lambda)$  increased with a rise in  $Ha$ . Fig. (3c) depicts that the nanoparticle volume fraction  $S(\lambda)$  reduces as  $Ha$  increases.

**Table 2** Convergence of HAM solutions for different order of approximations.

Order	$f(0.625)$	$\theta(0.625)$	$S(0.625)$
05	0.45201062040	0.80760004656	0.65436658412
10	0.45166547215	0.80760008211	0.65415106427
15	0.45133062142	0.80720010397	0.64106428731
20	0.44120618062	0.80720010598	0.64106337319
25	0.44120612487	0.80724016788	0.64105463192
30	0.44120612495	0.80722102382	0.64105463293
35	0.44120564124	0.80719025837	0.64105463524
40	0.44120564128	0.80719025389	0.64105467933
45	0.44120563244	0.80719024879	0.64105437932
50	0.44120563244	0.80719024689	0.64105437932
55	0.44120563244	0.80719024689	0.64105437932

This is due to the perpendicular effect of magnetite field on flow direction.

The variation of velocity  $f(\lambda)$ , temperature  $\theta(\lambda)$  and nanoparticle volume fraction  $S(\lambda)$  with Hall-parameter  $\beta_h$  is presented in Fig. (4). It is observed from Fig. (4a) that, the velocity increases with a raise in the parameter  $\beta_h$ . From Fig. (4b), it is noticed that, the dimensionless temperature  $\theta(\lambda)$  decreases with a raise in  $\beta_h$ . There is an enhancement in a nanoparticle concentration  $S(\lambda)$  with the rise in  $\beta_h$  as depicted in Fig. (4c). The inclusion of Hall parameter reduces the effective conductivity and hence drops the magnetic resistive force. Therefore, increase in  $\beta_h$  raises the velocity component  $f(\lambda)$ , the nanoparticle volume fraction  $S(\lambda)$  and decreases temperature  $\theta(\lambda)$ .

The variation of velocity in flow direction  $f(\lambda)$ , temperature  $\theta(\lambda)$  and nanoparticle volume fraction  $S(\lambda)$  with ion slip parameter  $\beta_i$  is presented in Fig. (5). It is observed from Fig. (5a) that the velocity enhances with the rise in the parameter  $\beta_i$ . Fig. (5b) reports that  $\theta(\lambda)$  decreases with the rise in  $\beta_i$ . There is an increment in the nanoparticle concentration  $S(\lambda)$  with an increase in  $\beta_i$  as depicted in Fig. (5c). The effective conductivity increases as increase in  $\beta_i$ , hence the damping force on the dimensionless velocity is decreasing due to this the dimensionless velocity increases.

The impact of the thermophoresis parameter  $Nt$  on dimensionless velocity  $f(\lambda)$ , temperature  $\theta(\lambda)$  and nanoparticle

**Table 1** Comparison of HAM for the velocity against analytical and SQLM for  $Gr = 0, Ha = 0, A = 0, Pr = 0, Nt = 0$  and  $Nb = 0$ .

$\lambda$	Sinha and Chaudhary (1966) analytical solution	Srinivasacharya and Himabindu (2016) SQLM	Present HAM
0.25	0	0	0
0.2684	0.02453	0.024532	0.0245333
0.3216	0.09546	0.095462	0.0954667
0.4046	0.20613	0.206127	0.206133
0.5091	0.34546	0.345462	0.345467
0.625	0.5	0.5	0.5
0.7409	0.65453	0.654539	0.654533
0.8454	0.793867	0.793863	0.793867
0.9284	0.90453	0.904529	0.904533
0.9816	0.97546	0.975468	0.975467
1	1	1	1



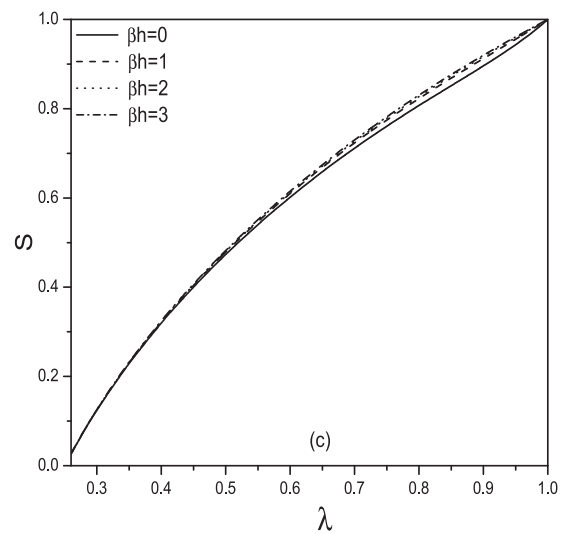
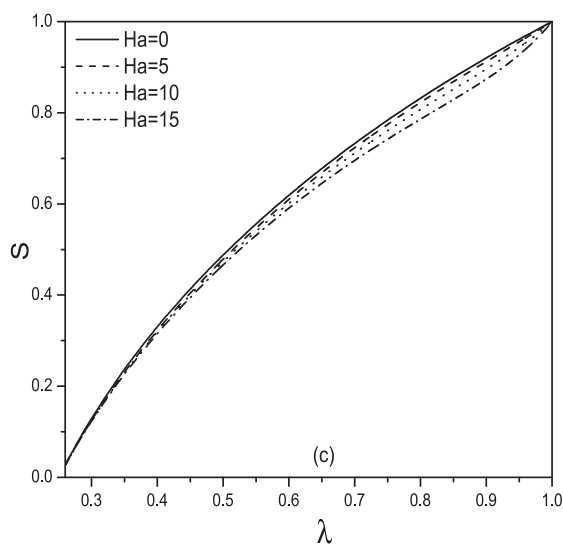
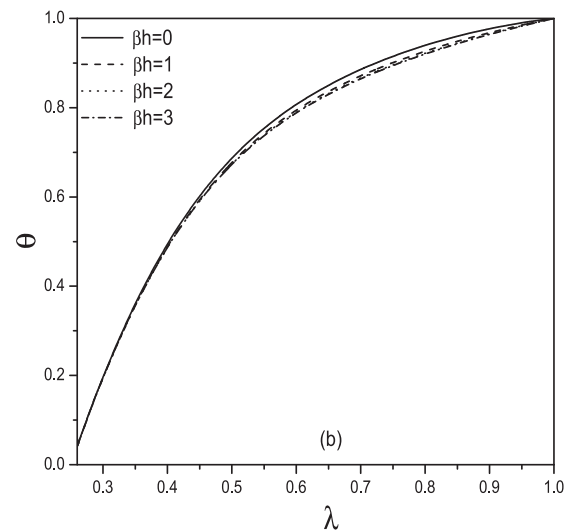
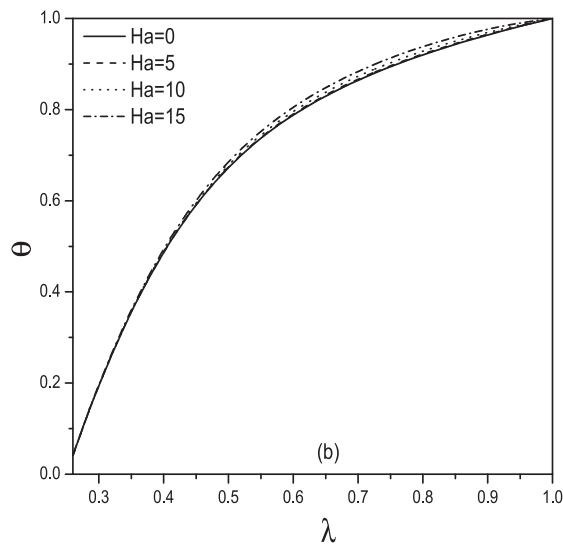
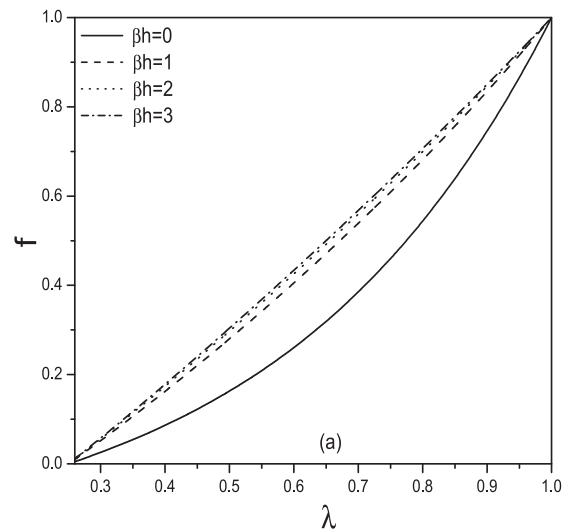
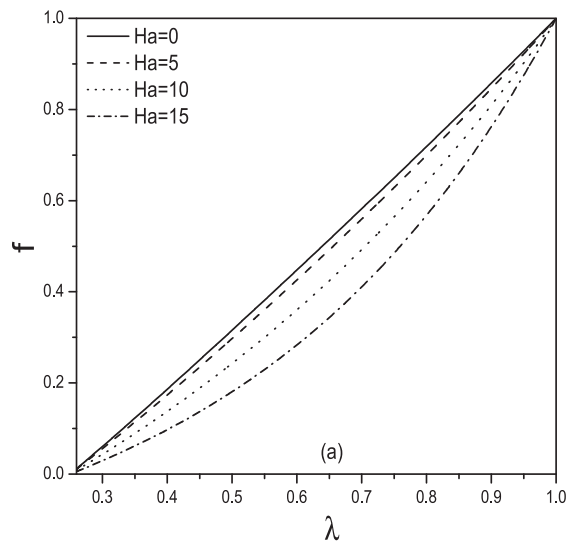


**Figure 3** Effect of  $Ha$  on (a) Velocity, (b) Temperature, (c) Nanoparticle concentration profiles.

**Figure 4** Effect of  $\beta_h$  on (a) Velocity, (b) Temperature, (c) Nanoparticle concentration profiles.

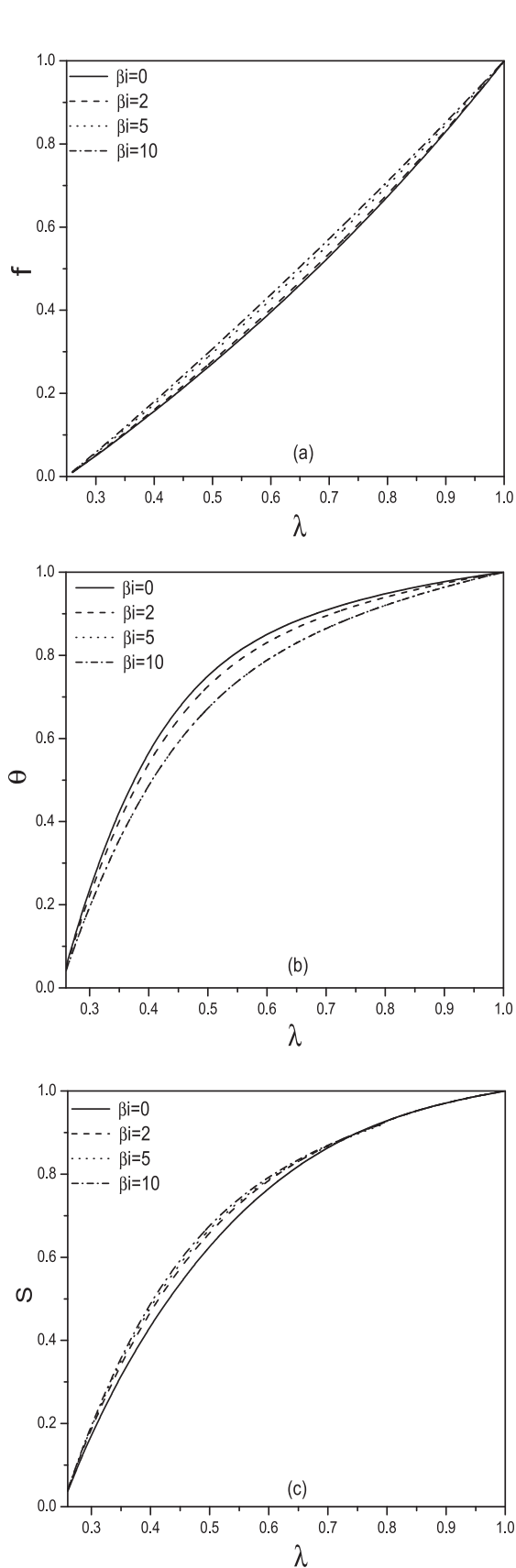


**Figure 5** Effect of  $\beta_i$  on (a) Velocity, (b) Temperature, (c) Nanoparticle concentration profiles.

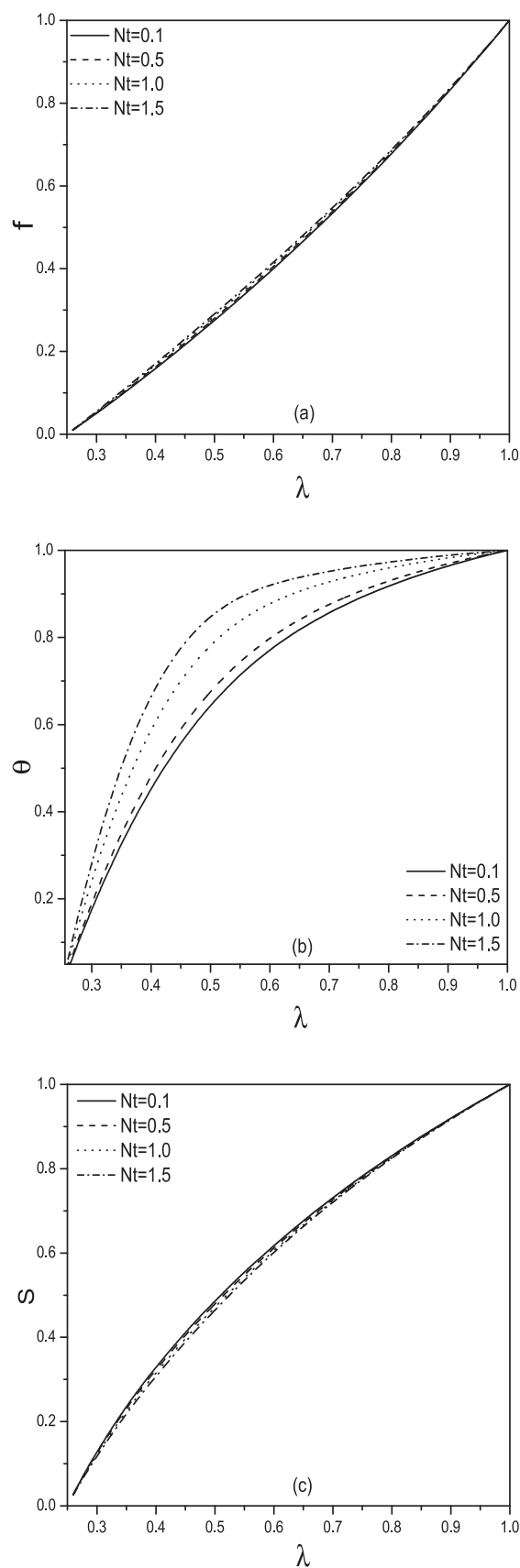


**Figure 6** Effect of  $Nt$  on (a) Velocity, (b) Temperature, (c) Nanoparticle concentration profiles.

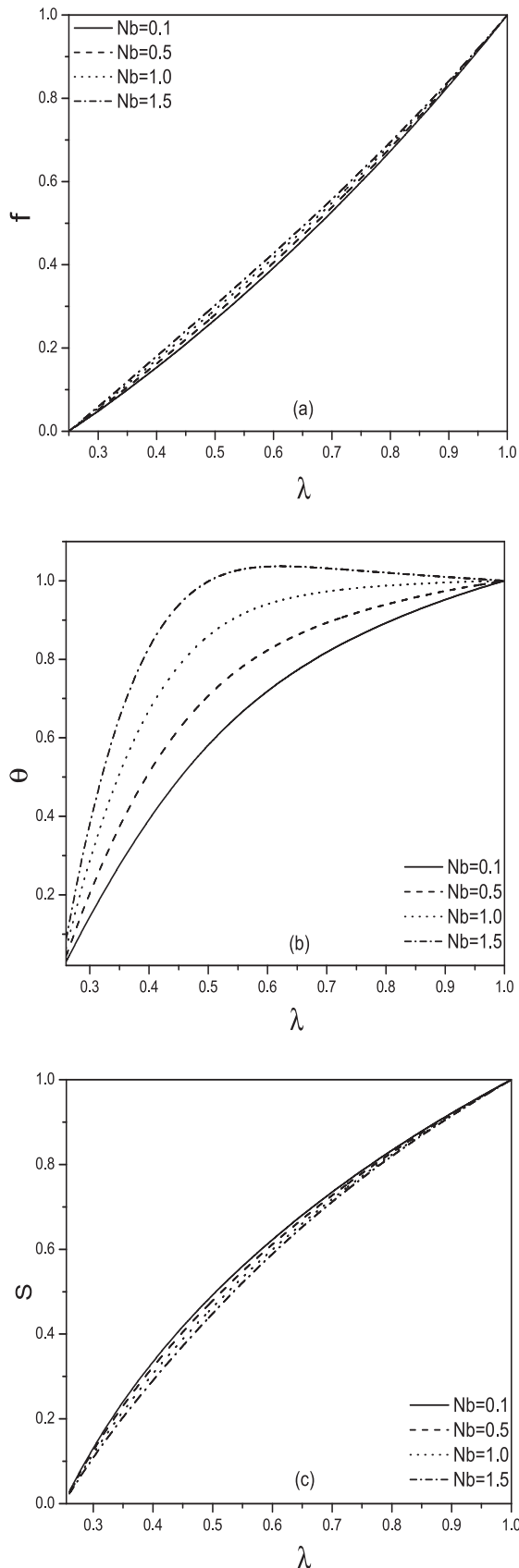


**Figure 7** Effect of  $Nb$  on (a) Velocity, (b) Temperature, (c) Nanoparticle concentration profiles.

concentration  $S(\lambda)$  is depicted in Fig. (6). The dimensionless velocity  $f(\lambda)$  raises with rise in  $Nt$  as shown in Fig. (6a). Fig. (6b) reveals that the  $\theta(\lambda)$  raises with a rise in parameter  $Nt$ . An increase in  $Nt$  leads to an increase in the effective-conductivity. It is recognized from Fig. (6c) that the nanoparticle concentration  $S(\lambda)$  decays with an increase in the value of  $Nt$ .

The influence of the Brownian motion  $Nb$  on the velocity  $f(\lambda)$ , dimensionless temperature  $\theta(\lambda)$  and nanoparticle concentration  $S(\lambda)$  is presented in Fig. (7). The velocity  $f(\lambda)$  raises with rise in  $Nb$  as shown in Fig. (7a). Fig. (7b) reveals that, the dimensionless temperature  $\theta(\lambda)$  enhances with enhancement in  $Nb$ . The nanoparticle volume fraction  $S(\lambda)$  decreases with an increase in  $Nb$  as depicted in Fig. (7c).

## 5. Conclusions

The present study investigates the influence of thermophoresis, Brownian motion, Hall and ion slip parameters on the mixed convective flow of nanofluid between the annuli of two concentric coaxial cylinders considering magnetic field. To solve the non-dimensional nonlinear equations using HAM procedure. The main observations are summarized below:

- As the magnetic parameter  $Ha$  increases the temperature increases whereas velocity and nanoparticle concentration decrease.
- As there is increment in Hall current, the velocity and the nanoparticle concentration increase but the temperature decreases.
- As ion slip parameter increases, the velocity and the nanoparticle concentration increase but the temperature decreases.
- As thermophoresis parameter increases, the velocity and temperature increase but the nanoparticle concentration decreases.
- As Brownian motion parameter increases, the velocity and temperature increase but the nanoparticle concentration decreases.

## References

- Akbar, S., Noreen, Raza M., Ellahi, R., 2015. Influence of induced magnetic field and heat flux with the suspension of carbon nanotubes for the peristaltic flow in a permeable channel. *Mag. Mater.* 381, 405–415.
- Ashorynejad, H.R., Abdulmajeed, A.M., Mohsen, S., 2013. Magnetic field effects on natural convection flow of a nanofluid in a horizontal cylindrical annulus using Lattice Boltzmann method. *Int. J. Therm. Sci.* 64, 240–250.
- Buongiorno, J., 2006. Convective transport in nanofluids, *ASME. J. Heat Transfer* 128, 240–250.
- Chamkha, A.J., Jena, S.K., Mahapatra, S.K., 2015. MHD convection of nanofluids – A review. *J. Nanofluids* 4 (3), 271–292.
- Choi, S.U.S., Eastman, J.A., 1995. Enhancing thermal conductivity of fluids with nanoparticles. *ASME Publ Fed*, New York 231, 99–106.
- Das, S., Chakraborty, S., Jana, R.N., Makinde, O.D., 2015. Mixed convective Couette flow of reactive nanofluids between concentric vertical cylindrical pipes. *J. Nanofluids* 4, 485–493.
- Dawood, H.K., Mohammed, H.A., Sidik, N.A.C., Munisamy, K.M., Wahid, M.A., 2015. Forced, natural and mixed-convection heat



- transfer and fluid flow in annulus: a review. *Int. Comm. Heat Mass Transfer* 62, 45–57.
- Ellahi, R., Mohsin, Hassan, Ahmad, Z., 2015. Study of natural convection MHD nanofluid by means of single and multi-walled carbon nanotubes suspended in a salt-water solution. *IEEE Trans. Nanotech.* 14 (4), 726–734.
- Ellahi, R., Hassan, M., Zeeshan, A., 2016. Aggregation effects on water base  $Al_2O_3$ -nanofluid over permeable wedge in mixed convection. *Asia-Pacific J. Chem. Eng.* 11 (2), 179–186.
- Garg, B.P., Singh, K.D., Bansal, A.K., 2014. Hall current effect on viscoelastic (Walters liquid model-B) MHD oscillatory convective channel flow through a porous medium with heat radiation. *Kragujevac J. Sci.* 36, 19–32.
- Hayat, T., Shafique, M., Tanveer, A., Alsaedi, A., 2016. Hall and ion slip effects on peristaltic flow of Jeffrey nanofluid with Joule heating. *J. Mag. Mag. Mater.* 407 (1), 51–59.
- Irfanullahkhan, S., Umar, K., Naveed, A., Saeed, U.J., Asif, W., Tauseefmohyuddin, S., 2015. Effects of viscous dissipation and convective boundary conditions on blasius and sakiadis problems for casson fluid. *Nat. Acad. Sci. Lett.* 38 (3), 247–250.
- Jamshad, A., Tauseefmohyuddin, S., 2014. An efficient technique for some highly nonlinear PDES in mathematical physics. *PLoS ONE* 9 (12).
- Kandelousi, M., Sheikholeslami, Ellahi, R., 2015. Simulation of ferrofluid flow for magnetic drug targeting using Lattice Boltzmann method. *J. Zeitschrift Fur Naturforschung, A* 70 (2), 115–124.
- Liao, S.J., 2003. *Beyond Perturbation, Introduction to Homotopy Analysis Method*. Publisher Taylor and Francis.
- Liao, S.J., 2004. On the homotopy analysis method for nonlinear problems. *Appl. Math. Comput.* 147 (2), 499–513.
- Liao, S.J., 2010. An optimal homotopy-analysis approach for strongly nonlinear differential equations. *Commun. Nonlinear Sci. Numer. Simul.* 15, 200–316.
- Liao, S.J., 2013. *Advances in the Homotopy Analysis Method*. World Scientific Publishing Company, Singapore.
- Mojtab, M., Shirvan, K.M., Ellahi, R., Asgar, B.R., 2016. Optimization of mixed convection heat transfer with entropy generation in a wavy surface square Lid-Driven cavity by means of Taguchi approach. *Int. J. Heat Mass Transfer* 102, 544–554.
- Mozayyeni, H.R., Rahimi, A.B., 2012. Mixed convection in cylindrical annulus with rotating outer cylinder and constant magnetic field with an effect in the radial direction. *Scientia Iranica B19* (1), 91–105.
- Naveed, A., Tauseefmohyuddin, S., Saleh, M.H., 2016. Flow and heat transfer of nanofluid in an asymmetric channel with expanding and contracting walls suspended by carbon nanotubes: a numerical investigation. *Aerosp. Sci. Tech.* 48, 53–60.
- Omid, M., Oztop, H., Pop, I., Mahmud, A., Wongwises, S., 2013. Entropy generation between two vertical cylinders in the presence of MHD flow subjected to constant wall temperature. *Int. Comm. Heat Mass Transfer* 44, 87–92.
- Rahman, S.U., Ellahi, R., Sohail, N., Zaigham, Z.Q.M., 2016. Simultaneous effects of nanoparticles and slip on Jeffrey fluid through tapered artery with mild stenosis. *J. Mol. Liquids* 218, 484–493.
- Rashidi, S., Dehghan, M., Ellahi, R., Riaz, M., Jamalabad, M.T., 2015. Study of stream wise transverse magnetic fluid flow with heat transfer around a porous obstacle. *J. Mag. Mag. Mater.* 378, 128–137.
- Sheikholeslami, M., Abelman, S., 2015. Two-phase simulation of nanofluid flow and heat transfer in an annulus in the presence of an axial magnetic field. *IEEE Trans. Nanotech.* 14 (3), 561–569.
- Sheikholeslami, M., Ellahi, R., 2015a. Electrohydrodynamic nanofluid hydrothermal treatment in an enclosure with sinusoidal upper wall. *Appl. Sci.* 5, 294–306.
- Sheikholeslami, M., Ellahi, R., 2015b. Three dimensional mesoscopic simulation of magnetic field effect on natural convection of nanofluid. *Int. J. Heat Mass Transfer* 89, 799–808.
- Sheikholeslami, M., Zaighamzia, Q.M., Ellahi, R., 2016. Influence of induced magnetic field on free convective heat transfer of nanofluid considering KKL correlation. *Appl. Sci.* 6 (11), 324.
- Sheikhzadeh, G.A., Teimouri, H., Mahmoodi, M., 2013. Numerical study of mixed convection of nanofluid in a concentric annulus with rotating inner cylinder. *Trans. Phenom. Nano Micro Scales* 1 (1), 26–36.
- Sinha, K.D., Chaudhary, R.C., 1966. Viscous incompressible flow between two coaxial rotating porous cylinders. *Proc. Nat. Inst. Sci.* 32, 81–87.
- Srinivasacharya, D., Himabindu, K., 2016. Entropy generation due to micropolar fluid flow between concentric cylinders with slip and convective boundary conditions. *Ain Shams Eng. J.* <http://dx.doi.org/10.1016/j.asej.2015.10.016>.
- Srinivasacharya, D., Kaladhar, K., 2012. Analytical solution of mixed convection flow of couple stress fluid between two circular cylinders with Hall and ion-slip effects. *Turkish. J. Eng. Environ. Sci.* 36, 226–235.
- Srinivasacharya, D., Kaladhar, K., 2013. Analytical solution for Hall and Ion-slip effects on mixed convection flow of Couple Stress fluid between parallel Discs. *Math. Comput. Modell.* 57, 2494–2509.
- Tani, I., 1962. Steady flow of conducting fluids in channels under transverse magnetic fields with consideration of Hall effects. *J. Aerosp. Sci.* 29, 297–305.
- Tauseefmohyuddin, S., Irfanullahkhan, S., 2016. Nonlinear radiation effects on squeezing flow of a Casson fluid between parallel disks. *Aerosp. Sci. Tech.* 48, 186–192.
- Tauseefmohyuddin, S., Zaidi, Zulfiqar Ali, Umar, K., Naveed, A., 2015. On heat and mass transfer analysis for the flow of a nanofluid between rotating parallel plates. *Aerosp. Sci. Tech.* 46, 514–522.
- Togun, H., Abdulrazzaq, T., Kazi, S.N., Badarudin, A., Kadhum, A. A.H., Sadeghinezhad, E., 2014. A review of studies on forced, natural and mixed heat transfer to fluid and nanofluid flow in an annular passage. *Renewable and Sustainable Energy Rev.* 39, 835–856.
- Umar, K., Naveed, A., Tauseefmohyuddin, S., 2015. Thermo-diffusion, diffusion-thermo and chemical reaction effects on MHD flow of viscous fluid in divergent and convergent channels. *Chem. Eng. Sci.* 141, 17–27.
- Umar, K., Naveed, A., Tauseefmohyuddin, S., 2016. Soret and Dufour effects on flow in converging and diverging channels with chemical reaction. *Aerosp. Sci. Tech.* 49, 135–143.
- Zulfiqar, A.Z.S., Tauseefmohyuddin, S., 2016. Convective heat transfer and MHD effects on two dimensional wall jet flow of a nanofluid with passive control mode. *Aerosp. Sci. Tech.* 49, 225–230.